

Extract from the lecture notes  
“Numerical Many Body Physics”

Wolfgang von der Linden (minor modification by E .Arrigoni)

Version vom March 15, 2010

# Contents

<b>1</b>	<b>Introduction</b>	<b>3</b>
<b>2</b>	<b>Many Body Hamiltonians</b>	<b>3</b>
2.1	Heisenberg model . . . . .	4
2.1.1	Spin 1/2 Heisenberg Antiferromagnet . . . . .	5
2.1.2	Matrix formulation and exact solution for two spins . . . . .	5
<b>3</b>	<b>Numeric representation</b>	<b>7</b>
3.1	Spin-1/2 systems . . . . .	7
3.1.1	Generation of basis states . . . . .	7
3.2	Computation of the Hamilton matrix . . . . .	8
3.3	Sparse matrices . . . . .	9
<b>4</b>	<b>Exact diagonalization</b>	<b>12</b>
4.1	The Power Method . . . . .	12
4.2	The Lanczos Method . . . . .	15
4.2.1	The poor man's Lanczos scheme . . . . .	15
4.2.2	Lanczos Method for Hermitean Matrices . . . . .	16
4.3	Dynamical Correlations . . . . .	20
4.3.1	Dynamic Green's functions . . . . .	20
4.3.2	Lehmann – Representation . . . . .	21

## 1 Introduction

The numerical treatment of many-body problems in solid state physics belongs to the realm of computer physics. Computer physics has evolved from 'number crunching' and 'dump data plotting' into a competitive field on a par with experimental and theoretical physics strongly entwined with both. Real experiments can be replaced by computer experiments as it is common practice in industry for monetary reasons. On the premises that an appropriate system is simulated, the numerical experiment is often much faster, less expensive and in some cases even the only feasible alternative. With little extra effort, system parameters can be modified and novel materials synthesized and their respective properties investigated.

As far as the links to theoretical physics are concerned the situation is similar. Computer physics has been disdained for many years by the 'pure theorists' claiming numerical results provide numbers and no insights. The situation has drastically changed over the last decade as testified by the significant and still increasing fraction of publications based essentially on computational techniques. Computer simulations from the theoretical viewpoint allow to scrutinize different models to figure out which fits the data best. Parameters can be modified with ease investigating wide parameter regimes with one and the same method. Otherwise different approaches have to be tailored for different parameter regimes, like weak coupling strong-coupling etc.

A widely used approach is the density functional theory in various guises. The most famous approximation is the Local density approximation with various approximations to the unknown exchange-correlation potential. By definition, these one-particle approaches describe weakly correlated systems. Strongly correlated many-body systems are defined as those in which the simultaneous presence of all particles is essential for the respective phenomena.

## 2 Many Body Hamiltonians

The genuine ab-initio Hamiltonian describing condensed matter is the ab-initio Hamilton operator containing in the Oppenheimer-approximation. It forms the starting point for bandstructure calculations in the local-density-approximation (LDA), in which electronic correlations are treated on a mean-field level. The realm of LDA calculations are weakly correlated systems, as opposed to strongly correlated electronic systems in which the detailed electron-electron-interaction is responsible for correlation effects such as antiferromagnetism, Kondo-effect, fractional quantum-hall effect, Mott-transition and many more.

An exact treatment of ab-initio many-body problems is illusory. There are two options, either we stick to the ab-initio many-body Hamiltonian and are satisfied with uncontrolled approximations or we resort to model Hamiltonians which hopefully still contain the crucial essentials of the sought-for physical effect.

Model systems have the advantage that they can either be solved exactly by

analytical means or they can be approached by numerical techniques. Numerical techniques are often the only feasible and reliable method for studying the really tough and long-standing problems of such systems.

In this lecture, we will not go through the more complicated models, such as the Hubbard or the Kondo model. For a detailed treatment, see [?]. Instead, we will stick on the most simple model that describes a correlated system, namely, the Heisenberg model.

## 2.1 Heisenberg model

The Hubbard type models describe itinerant electrons. If the charge degrees of freedom are bound to the atomic positions only the spin degrees of freedom remain active. They are described by the Heisenberg hamiltonian, the fundamental model in the theory of magnetism of local magnetic moments. It is defined by

$$H = \sum_{\langle i,j \rangle} J_{ij}^z S_i^z S_j^z + J_{ij}^\perp (S_i^x S_j^x + S_i^y S_j^y) + B \sum_i S_i^z \quad (1)$$

where  $S_i^\alpha$  ( $\alpha = x, y, z$ ) is the  $\alpha$ -th component of the spin-operator and  $J$  stands for the exchange integrals. The last term describes the coupling to an external magnetic field  $B$  in  $z$ -direction. This model is particularly geared for magnetic insulators like the 3d-,4d-,4f-,5f-systems. There are several special cases of the Heisenberg model

- $J^z = J^\perp$  ... isotropic Heisenberg model
- $J^\perp = 0$  ... Ising model
- $J^z = 0$  ... XY-model

The spin operators obey the well known commutator algebra

$$[S_i^\alpha, S_j^\beta] = i \delta_{i,j} \epsilon_{\alpha\beta\gamma} S_i^\gamma .$$

For numerical purposes it is convenient to introduce ladder operators

$$S_i^\pm = S_i^x \pm i S_i^y .$$

Therefore, the operators  $S^x$  and  $S^y$  can be written as

$$S_i^x = \frac{1}{2}(S_i^+ + S_i^-) \quad , \quad S_i^y = \frac{1}{2i}(S_i^+ - S_i^-) .$$

Instead of  $S^x$  and  $S^y$  we use the operators  $S^+$  and  $S^-$  to express the Hamiltonian

$$H = \sum'_{\langle i,j \rangle} \left\{ J_{ij} S_i^z S_j^z + \frac{1}{2} J_{ij}^\perp \underbrace{(S_i^+ S_j^- + S_i^- S_j^+)}_{F_{ij}} \right\} + B \sum_i S_i^z$$

where the summation is restricted to  $i \neq j$ .

### 2.1.1 Spin 1/2 Heisenberg Antiferromagnet

The isotropic ( $J = J^\perp$ ) spin-1/2 Heisenberg antiferromagnet ( $J > 0$ ) attracts particular interest as being the strong coupling limit of the Hubbard model at half-filling ( $N_\uparrow = N_\downarrow = N/2$ ) with  $J = 4t^2/U$  [1]. Moreover, it is governed by quantum effects more than any other spin system.

However, the perfectly ordered Neel-state  $|\uparrow\downarrow\uparrow\downarrow\rangle$  is not the ground state of the system.

The Hamiltonian has the special form

$$H = \sum_{\langle ij \rangle} \left\{ JS_i^z S_j^z + \frac{J^\perp}{2} F_{ij} \right\}. \quad (2)$$

We have used the common sign convention for the exchange-integral. In the antiferromagnetic case  $J$  is negative. The spin-spin interaction is restricted to nearest-neighbor sites, indicated by  $\langle ij \rangle$ . The so-called flip operator  $F_{ij}$  has a simple meaning for spin-1/2 particles. It swaps the spin-values of the neighboring sites  $i$  and  $j$ , if the spins have opposite sign. Otherwise, the application of  $F_{ij}$  yields the null vector.

$$\hat{F}_{i,j} |\dots, \sigma_i, \dots, \sigma_j, \dots\rangle = \begin{cases} |\dots, -\sigma_i, \dots, -\sigma_j, \dots\rangle & \text{if } \sigma_i = -\sigma_j, \\ 0 & \text{otherwise.} \end{cases} \quad (3)$$

### 2.1.2 Matrix formulation and exact solution for two spins

The Hilbert space of the many body system is given by the tensor product of the Hilbert space of each single site.

To make an example, for a spin  $\frac{1}{2}$ , the Hilbert space for a single spin is spanned by the basis elements

$$\left\{ |\sigma\rangle, \sigma = \pm\frac{1}{2} \right\} = \left\{ \left| +\frac{1}{2} \right\rangle, \left| -\frac{1}{2} \right\rangle \right\}.$$

For  $N$  spins (on  $N$  sites) the Hilbert space is spanned by the basis

$$\left\{ |\sigma_1, \dots, \sigma_N\rangle, \sigma_1 = \pm\frac{1}{2}, \dots, \sigma_N = \pm\frac{1}{2} \right\}.$$

For  $N = 2$ , we have four elements, which we denote as

$$|1\rangle \equiv \left| -\frac{1}{2}, -\frac{1}{2} \right\rangle, |2\rangle \equiv \left| \frac{1}{2}, -\frac{1}{2} \right\rangle, |3\rangle \equiv \left| -\frac{1}{2}, \frac{1}{2} \right\rangle, |4\rangle \equiv \left| \frac{1}{2}, \frac{1}{2} \right\rangle$$

The matrix elements  $\langle x|H|x'\rangle$  can be easily computed with the help of (2),

leading to the *matrix representation* of the Hamiltonian

$$H = \begin{pmatrix} \frac{J}{4} & 0 & 0 & 0 \\ 0 & -\frac{J}{4} & \frac{J^\perp}{2} & 0 \\ 0 & \frac{J^\perp}{2} & -\frac{J}{4} & 0 \\ 0 & 0 & 0 & \frac{J}{4} \end{pmatrix} \quad (4)$$

This matrix can be easily diagonalized. Two eigenvalues can be identified at once as being  $\frac{J}{4}$ . The other two can be obtained by a simple diagonalisation of the  $2 \times 2$  matrix in the center, and are given by  $-\frac{J}{4} \pm \frac{J^\perp}{2}$ .

The fact that the Hilbert space splits up into three sectors, which are not admixed by the Hamiltonian is no accident. The three sectors correspond to states with fixed value  $S_z$  of the  $z$ -component of the total spin, which is equal to  $\pm 1$  and to  $0$ , respectively. This symmetry of the Hamiltonian (together with, possibly, further ones) should be exploited in numerical treatments as well.

Upon increasing the number  $N$  of sites (spins) the problem becomes much more complex, and at some point it cannot be treated analytically any more. The dimension of the Hilbert space (and thus the size of the matrix) becomes  $2^N$ . Therefore one has to diagonalize a  $2^N \times 2^N$  matrix. Already for  $N$  not too large, memory requirements become prohibitive. For  $N = 16$  one needs  $\approx 10$  Gygabytes of memory.

It is characteristic of a many-body problem that its complexity increases *exponentially*, this is the reason why it is a difficult task.

Notice that even exploiting the conservation of  $S_z$ , and writing a matrix restricted to the states with a fixed  $S_z = 0$  (say), the dimension of the Hilbert space would be

$$\frac{N!}{(N/2)!(N/2)!} \rightarrow 2^N$$

which is again exponentially large.

### 3 Numeric representation

There are four prerequisites a basis set should fulfill:

- It must be rapidly generated
- matrix elements are easy to compute
- modest need of memory
- fast access of states.

We will discuss the best basis sets and their numerical representation for spin systems.

#### 3.1 Spin-1/2 systems

Instead of the two spin values  $\sigma = \pm\frac{1}{2}$  we use the integers  $n_i = \frac{\sigma_i+1}{2} \in \{0, 1\}$ . One is prompted to identify the sequence of  $n_i$  values as bit-pattern of the integer  $I = \sum_{i=1}^N n_i 2^{i-1}$ . For instance the basis state  $|\psi\rangle = |-\frac{1}{2}, +\frac{1}{2}, -\frac{1}{2}, +\frac{1}{2}\rangle$  is represented by  $n = \{0101\}$ , which again is mapped onto the integer 5. This representation has two advantages, it keep the memory requirements as small as possible and it speeds up certain numerical operations.

As already mentioned, since  $S^z = \sum_{i=1}^N S_i^z$  commutes with the Hamiltonian, the Hamilton matrix is block-diagonal in the sectors with fixed  $S^z$  values, i.e. fixed numbers  $N^\sigma$  of  $\sigma$ -spins. For a given  $S^z$ -sector the number of ones in the bit-pattern is fixed, which reduces the number of basis states to

$$L = \binom{N}{N^\uparrow}, \tag{5}$$

where  $N$  is the number of lattices sites and

$$S^z = \frac{1}{2} 2N^\uparrow - N.$$

For instance, if the number of sites is  $N = 16$  there are  $2^{16} = 65536$  possible basis states in total, whereas there are merely  $\binom{16}{8} = 12870$  for  $S^z = 0$ , i.e.  $N^\uparrow = N^\downarrow = 8$ , which is much less. Translation and Spin Rotation (when applicable) could also be exploited which would reduce the number of basis state even further.

##### 3.1.1 Generation of basis states

For fixed  $N^\uparrow$  not all integer values represent a permissible configuration, since the number of ones and zeros in the bit-pattern are fixed. We generate the basis

states in such a way that the corresponding integer values are in increasing order. The basis states and their integer representations are therefore

$$\begin{aligned}
|\varphi_1\rangle &= \{ \overbrace{0, 0, \dots, 0}^{N-N^\dagger}, \overbrace{0, 1, 1, 1, \dots, 1}^{N^\dagger} \}; & I_1 &= 2^{N^\dagger} - 1 \\
|\varphi_2\rangle &= \{ 0, 0, \dots, 0, 1, 0, 1, 1, \dots, 1 \}; & I_2 &= 2^{N^\dagger+1} - 1 - 2^{N^\dagger-1} \\
|\varphi_3\rangle &= \{ 0, 0, \dots, 0, 1, 1, 0, 1, \dots, 1 \}; & I_3 &= 2^{N^\dagger+1} - 1 - 2^{N^\dagger-2} \\
&\vdots & & \\
|\varphi_L\rangle &= \{ \overbrace{1, 1, 1, \dots, 1}^{N^\dagger}, \overbrace{0, 0, \dots, 0}^{N-N^\dagger} \}; & I_L &= 2^N - 2^{N-N^\dagger}.
\end{aligned}$$

In practice, thus, one stores a length- $L$  array  $b(1 : L)$  of integers, where  $b(\nu) = I_\nu$ . The element  $\nu$  of the array contains the decimal representation of the bit sequence describing the basis state  $|\varphi_\nu\rangle$ . As an example we consider a four-site cluster with  $S^z = 0$ , i.e. two up and two down spins.

$\nu$	1	2	3	4	5	6
bit	0011	0101	0110	1001	1010	1100
$I_\nu$	3	5	6	9	10	12
storage	b(1)=3	b(2)=5	b(3)=6	b(4)=9	b(5)=10	b(6)=12

Table 1: *Example for the representation of spin pattern as integers.*

When evaluating matrix elements, it is necessary, for a given bit sequence  $b_0$ , to find the corresponding  $\nu$ , such that  $b(\nu) = b_0$ . The advantage of ordered basis states ( $b(\nu)$  is an increasing function of  $\nu$ ), is that  $\nu$  can be efficiently searched by bisection.

### 3.2 Computation of the Hamilton matrix

Here we want to compute the matrix elements

$$h_{\nu'\nu} = \langle \Phi_{\nu'} | H | \Phi_\nu \rangle \quad (6)$$

of the Hamiltonian in suitable basis states  $|\Phi_\nu\rangle$ . To this end we split the Hamiltonian into individual contributions  $H^{(l)}$

$$H = \sum_{l=1}^{N_i} H^{(l)} \quad (7)$$

such that the application of one such term  $H^{(l)}$  to a basis state  $|\Phi_\nu\rangle$  yields again a basis state or the null vector, i.e.

$$H^{(l)} |\Phi_\nu\rangle = h_{\nu'\nu}^{(l)} |\Phi_{\nu'}\rangle. \quad (8)$$

The full matrix element  $\langle \Phi_{\nu'} | H | \Phi_{\nu} \rangle$  is obtained by summing up all contributions  $h_{\nu'\nu}^{(l)}$ . Clearly, if there is only one term  $H^{(l)}$  in Hamiltonian that mediates between the two basis states  $|\Phi_{\nu}\rangle$  and  $|\Phi_{\nu'}\rangle$ , then  $h_{\nu'\nu} = h_{\nu'\nu}^{(l)}$ . As an example we consider the antiferromagnetic Heisenberg model (2) in the real-space basis (??), characterized by the set of “occupation numbers”  $|\Phi_{\nu}\rangle = |\{n_i^{(\nu)}\}\rangle$  for all lattice sites  $i$  with  $n_i^{(\nu)} \in \{0, 1\}$ .

The  $S_z S_z$  part proportional to  $J$  (2) is diagonal in this basis, so we have

$$h_{\nu\nu} = J \sum_{\langle ij \rangle} (n_i^{(\nu)} - \frac{1}{2})(n_j^{(\nu)} - \frac{1}{2}) \quad (9)$$

There are no other contributions to the diagonal elements.

For the off-diagonal terms, an individual contribution is given for an  $F_{ij}$  for a given pair of nearest-neighbor terms.

$$H^{(l)} = \frac{J^{\perp}}{2} F_{i_0 j_0} \quad (10)$$

Application of one of these terms,  $H^{(l)}$  say, to a basis state  $|\Phi_{\nu}\rangle = |\{n_i^{(\nu)}\}\rangle$  results either in the null vector, if  $n_{i_0}^{(\nu)} = n_{j_0}^{(\nu)}$ , Otherwise, the spin-flip process is possible and results in another basis state  $|\Phi_{\nu'}\rangle = |\{n_i^{(\nu')}\}\rangle$  which differs from  $|\Phi_{\nu}\rangle$  only in the exchange of the “occupation numbers”  $n_{i_0}^{(\nu)}$  and  $n_{j_0}^{(\nu)}$ , i.e.

$$\begin{aligned} n_i^{(\nu')} &= n_i^{(\nu)} & \forall i \neq i_0, j_0 \\ n_{i_0}^{(\nu')} &= n_{j_0}^{(\nu)} \\ n_{j_0}^{(\nu')} &= n_{i_0}^{(\nu)}. \end{aligned} \quad (11)$$

There is only one spin-flip process  $H^{(l)}$  mediating between the two basis states under consideration. The respective matrix element is therefore

$$h_{\nu'\nu} = \begin{cases} \frac{J^{\perp}}{2} & \text{if (11) is fulfilled,} \\ 0 & \text{otherwise.} \end{cases} \quad (12)$$

### 3.3 Sparse matrices

In the above-mentioned representation the many-body Hamilton-matrices  $H_{\nu\nu'}$  are sparse. We have seen that only a small fraction of all matrix elements is not zero. It is sensible to store only the nonzero matrix elements not only to save memory but also to speed up operations of the form  $H\mathbf{x}$  which form the heart of the exact diagonalization schemes that will be discussed in the next chapter.

In our case, as discussed in 3.2, we split, the Hamiltonian in pieces  $H^{(l)}$ , such that, for a given  $\nu$  there is at most one  $\nu'$  such that  $H_{\nu\nu'}^{(l)} \neq 0$ . Accordingly, it

is convenient to split the Hamiltonian matrix into terms connecting two indices only:

$$H(\nu, \nu') = \sum_{nz=1}^{N_{nz}} H_c(nz) \delta_{\nu, \nu(nz)} \delta_{\nu', \nu'(nz)}$$

In this way, we only need to store one real and two integer arrays of length  $N_{nz}$ , namely  $H_c(1 : N_{nz}), \nu(1 : N_{nz}), \nu'(1 : N_{nz})$ . The advantage is that  $N_{nz}$  is typically of order  $L$  instead of  $L^2$ . Therefore, we can write the algorithm to store sparse matrices as

---

**Algorithm 3.1:** COMPACT STORAGE( $H, H_c, ind, N_{nz}$ )

---

**initialize:**

$$\begin{aligned} L &= \text{size}(H) \\ N_{nz} &= 0 \end{aligned}$$

**do**  $\nu = 1, L$

**do**  $l = 1, N_l$

**if**  $H^{(l)} |\Phi_\nu\rangle \neq 0$  (see (8)) **then**

      determine the corresponding (unique)  $\nu'$  and  $h_{\nu, \nu'}^{(l)}$

$$N_{nz} = N_{nz} + 1$$

$$H_c(N_{nz}) = h_{\nu, \nu'}^{(l)}$$

$$ind(N_{nz}, 1) = \nu$$

$$ind(N_{nz}, 2) = \nu'$$

**endif**

**end do**

**end do**

---

The only operation the matrix will be used for is action on a vector. The compact storage can directly be used to perform only the nonzero multiplications

as depicted in the following algorithm

---

**Algorithm 3.2:** MULTIPLY H  $\mathbf{x}(H_c, ind, N_{nz}, \mathbf{x}, \mathbf{y})$

---

**initialize:**

$\mathbf{y} = 0$

**do**  $i = 1, N_{nz}$

$i_1 = \text{ind}(i, 1)$

$i_2 = \text{ind}(i, 2)$

$y(i_1) = y(i_1) + H_c(i) * x(i_2)$

**end do**

---

## 4 Exact diagonalization

In this chapter we describe methods for the exact evaluation of eigenvalues and eigenvectors of many-body Hamiltonians. There are very powerful exact diagonalization algorithms in the textbooks about numerical mathematics. A severe drawback of these schemes is their limitation to matrix sizes of the order  $N = O(10^3)$ . Strongly correlated many-body problems, however, start with  $N = O(10^8)$  and go way beyond. It is obvious that conventional schemes are powerless in these cases. On the other hand, for the *full diagonalisation* of *generic* hermitian matrices, standard methods are more appropriate.

The point is that, since the interesting quantum features of strongly correlated many-body systems show up at very low temperatures, merely the ground-state and a few low-lying eigenvalues and the corresponding eigenvectors are required. In addition, for most systems an appropriate basis can be found, in which the Hamilton-matrices are sparse. The number of nonzero matrix elements is typically  $O(N)$  rather than  $O(N^2)$ .

A standard scheme from numerical mathematics, which allows to take advantage of the sparseness of a matrix and which allows to concentrate on the groundstate only, is the so-called power method or rather the vector-iteration due to von Mises.

### 4.1 The Power Method

The Power method is a simple and yet powerful technique to determine the eigenvector corresponding to the “dominant” eigenvalue. The eigenvalue problem for the Hamilton operator  $H$  under consideration reads

$$\hat{H} |\varphi_l\rangle = \epsilon_l |\varphi_l\rangle \quad \text{with} \quad \langle \varphi_l | \varphi_{l'} \rangle = \delta_{l,l'} \quad (13)$$

with real eigenvalue  $\epsilon_l$  and mutually orthogonal and normalized eigenvectors  $|\varphi_l\rangle$ . The eigenvalues may be degenerate. The idea, as the name says, is to apply high “powers” of the Hamiltonian to a starting states, such that the components of the initial states with largest energies (in absolute values) increase with respect to the other ones. One can “target” different states by introducing a spectral shift

$$\hat{H} \rightarrow \hat{H}' = \hat{H} - E_s \hat{I} \quad \text{and} \quad \epsilon_l \rightarrow \epsilon'_l = \epsilon_l - E_s ,$$

which does not affect the eigenvectors  $|\varphi_l\rangle$ . Therefore, we can adapt  $E_s$  in such a way that the ground state yields the dominant eigenvalue, i.e.

$$|\epsilon'_0| \geq |\epsilon'_l| \quad \forall l .$$

To ensure that the groundstate energy  $\epsilon'_0$  has the greatest modulus of all eigenvalues the condition

$$\epsilon'_0 < -\frac{W}{2} \equiv -\frac{\epsilon_N - \epsilon_0}{2}$$

has to be fulfilled, which yields the condition

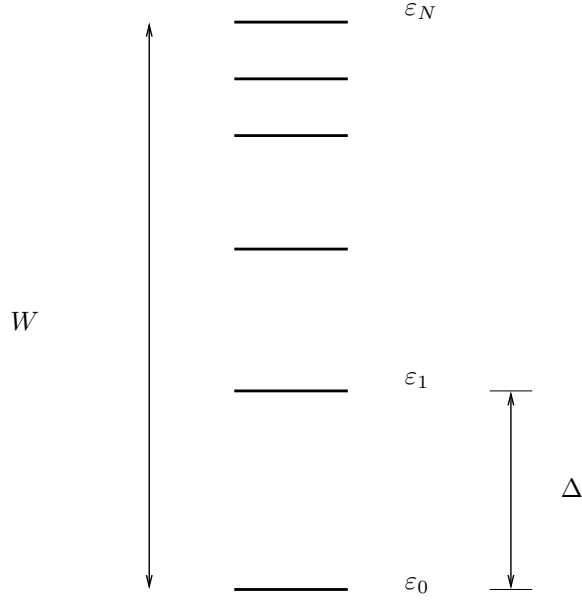


Figure 1: Schematic representation of the eigenvalues of the Hamiltonian. The gap between the lowest two eigenvalues is denoted by  $\Delta$

$$E_s > \frac{\epsilon_0 + \epsilon_N}{2} .$$

Next we want to apply the Power method to  $\hat{H}'$  starting with an initial vector

$$|x_0\rangle = \sum_{l=0}^N |\varphi_l\rangle \underbrace{\langle \varphi_l | x_0 \rangle}_{c_l} .$$

chosen at random, possibly subject to suitable symmetry constraints. After  $n$  repeated applications of  $\hat{H}'$  we obtain

$$|\tilde{x}_n\rangle \stackrel{\text{def}}{=} \hat{H}'^n |x_0\rangle = \sum_{l=0}^N |\varphi_l\rangle c_l \epsilon_l'^n , \quad (14)$$

This illustrates what anticipated above. The normalization yields

$$|x_n\rangle \stackrel{\text{def}}{=} \frac{|\tilde{x}_n\rangle}{\| \tilde{x}_n \|} = \frac{\sum_l c_l \epsilon_l'^n |\varphi_l\rangle}{\left( \sum_l |c_l|^2 \epsilon_l'^{2n} \right)^{1/2}} = \frac{\sum_l \frac{c_l}{c_0} \left( \frac{\epsilon_l'}{\epsilon_0'} \right)^n |\varphi_l\rangle}{\left( \sum_l \left( \frac{c_l}{c_0} \right)^2 \left( \frac{\epsilon_l'}{\epsilon_0'} \right)^{2n} \right)^{1/2}} .$$

Since  $\left( \frac{\epsilon_l'}{\epsilon_0'} \right) < 1$ , it is clear that for large  $n$ ,  $\left( \frac{\epsilon_l'}{\epsilon_0'} \right)^n$  becomes arbitrarily small. Assuming that the groundstate energy is not degenerate and the initial vector

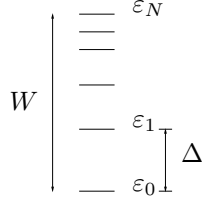


Figure 2: Schematic representation of the eigenvalues of the Hamiltonian. The gap between the lowest two eigenvalues is denoted by  $\Delta$

has a non-vanishing overlap with the sought-for groundstate, the Power method converges to the true groundstate

$$|x_n\rangle = |\varphi_0\rangle + O(q^n) \xrightarrow{n \rightarrow \infty} |\varphi_0\rangle .$$

where we have introduced

$$q \stackrel{\text{def}}{=} \max_i \left| \frac{\varepsilon'_i}{\varepsilon'_0} \right| .$$

If the initial vector is orthogonal to the groundstate, the iteration converges to the lowest eigenstate which has a non-vanishing contribution in  $|x_0\rangle$ . This can be used directly to determine states with given symmetry, e.g. the dispersion relation of the lowest excitations.

The ratio  $q$  is either  $\left| \frac{\varepsilon'_1}{\varepsilon'_0} \right|$  or  $\left| \frac{\varepsilon'_N}{\varepsilon'_0} \right|$ . The best convergence is achieved if

$$\left| \frac{\varepsilon'_1}{\varepsilon'_0} \right| = \left| \frac{\varepsilon'_N}{\varepsilon'_0} \right| \Rightarrow q = \left| \frac{1 - \Delta/W}{1 + \Delta/W} \right| .$$

Obviously, the convergence is governed by the ratio  $\Delta/W$ . The closer the excited states is to the groundstate, the longer it takes to get rid of its contribution in  $|x_n\rangle$ .

If the lowest eigenvalue is degenerate

$$\varepsilon'_0 = \varepsilon'_1 = \dots = \varepsilon'_L < \varepsilon_{L+1}$$

then then the Power iterate  $|x_n\rangle$  converge towards the projection of the initial vector  $|x_0\rangle$  onto the eigenspace of the first eigenvalue:

$$|x_n\rangle \xrightarrow{n \rightarrow \infty} \frac{\mathbb{P}|x_0\rangle}{\langle x_0|\mathbb{P}|x_0\rangle}$$

where  $\mathbb{P}$  is the projector onto the eigenspace of the ground state

$$\mathbb{P} = \sum_{l=0}^L |\varphi_l\rangle\langle\varphi_l| .$$

Using the expansion (14) for the energy-expectation value

$$\langle x_n | \hat{H} | x_n \rangle = \epsilon_0 + O\left(|\epsilon_1/\epsilon_0|^{2n}\right)$$

shows that the energy converges faster than the vector  $|x_n\rangle$ .

On passing we note that the power-method allows also to determine excited states. Once the ground state is approximately determined a new sequence of iterations is started with an initial vector orthogonal to the approximate groundstate. Since the groundstate is approximate and due to the presence of numerical noise, the vectors  $\mathbf{x}_n$  loose the orthogonality to the ground with increasing number of iterations and it is expedient to re-orthogonalize the vectors once in a while.

## 4.2 The Lanczos Method

The Power method uses only a small part of the information actually provided by the power method. One can do much better with only a little more computational effort. This goal is achieved by the *Lanczos method*.

### 4.2.1 The poor man's Lanczos scheme

To begin with, we analyze the information content of the first Power method iteration. After one step we have two normalized vectors  $|x_0\rangle$  and  $|x_1\rangle$ , which are in general not orthogonal, and the corresponding energy-expectation values are

$$E_0^P = \langle x_0 | \hat{H} | x_0 \rangle$$

$$E_1^P = \langle x_1 | \hat{H} | x_1 \rangle .$$

The basic idea of the Lanczos method is to diagonalize the Hamiltonian in the subspace spanned by  $\{|x_0\rangle, |x_1\rangle\}$ , i.e. to minimize the energy of the variational Ansatz

$$|x_1^L\rangle = \alpha |x_0\rangle + \beta |x_1\rangle$$

$$E_1^L = \min_{\alpha, \beta} \frac{\langle x_1^L | H | x_1^L \rangle}{\langle x_1^L | x_1^L \rangle} \leq \langle x_1 | H | x_1 \rangle .$$

The last inequality follows since  $\langle x_1 | H | x_1 \rangle$  corresponds to the special case  $\alpha = 0, \beta = 1$ . It can easily be shown that the energy of the Lanczos method is actually lower than that of the Power method provided  $\langle x_1 | \hat{H} | x_0 \rangle \neq 0$ . This procedure can be repeated by choosing the Lanczos vector  $|x_1^L\rangle$  as initial vector of the subsequent iteration. The results of the Power method are

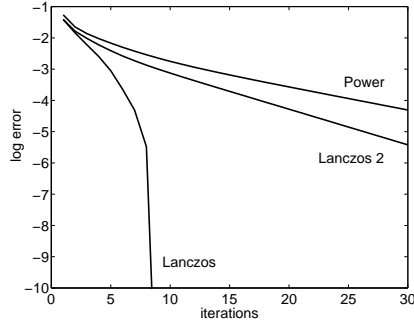


Figure 3: Comparison of the speed of convergence to the exact ground-state energy of the Power method and the Lanczos method. Lanczos 2 stands for the introductory example of only two vectors

compared with those of the simple Lanczos scheme for a  $10 \times 10$  tight binding matrix.

$$H = \begin{pmatrix} -1 & 1 & 0 & \cdot & \cdot \\ 1 & -1 & 1 & 0 & \cdot \\ \cdot & 1 & -1 & 1 & 0 \\ \cdot & \cdot & 1 & -1 & 1 \\ \cdot & \cdot & \cdot & 1 & \ddots \end{pmatrix}$$

where an appropriate spectral shift has been introduced. The energies are depicted in Fig. 3. Obviously, the 'poor man's lanczos' scheme (Lanczos 2) is superior, but not overwhelmingly so. Particularly disturbing is the observation, that it takes more than 10 iterations, which is the dimension of the matrix, to achieve convergence.

It is, however, straight forward, to generalize and improve the above ideas. Instead of taking only two vectors into account, we keep all vectors  $|x_n\rangle$ , generated during the iterations of the Power method. The set of vectors  $|x_n\rangle$  spans the  $n$ -dimensional so-called Krylov space. The minimization of the variational energy leads to the generalized eigenvalue problem depending on the matrix elements of the Hamiltonian and on the overlap matrix of the vectors  $|x_n\rangle$ . Linear dependencies of these basis states can lead to severe numerical problems. It is therefore better to transform the basis set  $\{|x_n\rangle\}$  into an orthonormal set of vectors that still spans the Krylov space.

#### 4.2.2 Lanczos Method for Hermitean Matrices

The Lanczos procedure starts with an appropriate normalized initial vector  $|x_0\rangle$ , chosen along the lines outlined before. The corresponding energy-expectation value is

$$\varepsilon_0 = \langle x_0 | \hat{H} | x_0 \rangle.$$

Next we apply the Hamiltonian to  $|x_0\rangle$  in order to determine the next basis vector

$$|\tilde{x}_1\rangle = \hat{H}|x_0\rangle - \varepsilon_0|x_0\rangle.$$

Since the vectors have been orthogonalized à la Gram-Schmidt

$$\langle x_0|\tilde{x}_1\rangle = 0$$

and the vector is normalized

$$|x_1\rangle = \frac{|\tilde{x}_1\rangle}{\| \tilde{x}_1 \|}$$

The next basis vector is generated using the prescription (again Gram-Schmidt)

$$|\tilde{x}_2\rangle = H|x_1\rangle - \varepsilon_1|x_1\rangle - k_1|x_0\rangle$$

We choose the coefficients  $\varepsilon_1$  and  $k_1$  such that  $|\tilde{x}_2\rangle$  is orthogonal to the previous basis vectors  $\{|x_0\rangle, |x_1\rangle\}$ :

$$\langle x_1|\tilde{x}_2\rangle = \langle x_1|\hat{H}|x_1\rangle - \varepsilon_1 - k_1 \underbrace{\langle x_1|x_0\rangle}_{=0} = 0$$

$$\langle x_0|\tilde{x}_2\rangle = \langle x_0|\hat{H}|x_1\rangle - \varepsilon_1 \underbrace{\langle x_0|x_1\rangle}_{=0} - k_1 = 0$$

Hence,  $\varepsilon_1$  is again the expectation value,

$$\varepsilon_1 = \langle x_1|\hat{H}|x_1\rangle \text{ and } k_1 = \langle x_0|\hat{H}|x_1\rangle.$$

By construction, the quantity  $k_1$  is real, since

$$k_1^* = \langle x_1|\hat{H}|x_0\rangle = \langle x_1|\tilde{x}_1\rangle + \varepsilon_0 \underbrace{\langle x_1|x_0\rangle}_{=0} = \|\tilde{x}_1\| \in \mathbb{R}.$$

We add the normalized vector  $|\tilde{x}_2\rangle$  to the set of orthonormal basis states  $\{|x_0\rangle, |x_1\rangle, |x_2\rangle\}$ .

The procedure continues in the same way: assuming that we have already generated a set of  $n+1$  mutually orthonormal vectors  $\{|x_0\rangle, |x_1\rangle, \dots, |x_n\rangle\}$ . The next vector  $|x_{n+1}\rangle$  is determined as follows

$$|\tilde{x}_{n+1}\rangle = \hat{H}|x_n\rangle - \varepsilon_n|x_n\rangle - k_n|x_{n-1}\rangle$$

$$\varepsilon_n = \langle x_n|\hat{H}|x_n\rangle$$

$$k_n = \langle x_{n-1}|\hat{H}|x_n\rangle = \|\tilde{x}_n\|$$

$$|x_{n+1}\rangle = \frac{|\tilde{x}_{n+1}\rangle}{\|\tilde{x}_{n+1}\|}.$$

One can see that  $|x_{n+1}\rangle$  is orthogonal to all previous vectors .

$$\begin{aligned}\langle x_n | \tilde{x}_{n+1} \rangle &= \underbrace{\langle x_n | \hat{H} | x_n \rangle}_{\varepsilon_n} - \varepsilon_n \underbrace{\langle x_n | x_n \rangle}_{=1} - k_n \underbrace{\langle x_n | x_{n-1} \rangle}_{=0} = 0 \\ \langle x_{n-1} | \tilde{x}_{n+1} \rangle &= \underbrace{\langle x_{n-1} | \hat{H} | x_n \rangle}_{k_n} - \varepsilon_n \underbrace{\langle x_{n-1} | x_n \rangle}_{=0} - k_n \underbrace{\langle x_{n-1} | x_{n-1} \rangle}_{=1} = 0\end{aligned}$$

For  $i = 1, \dots, n-2$  we have

$$\langle x_i | \tilde{x}_{n+1} \rangle = \langle x_i | \hat{H} | x_n \rangle - \varepsilon_n \underbrace{\langle x_i | x_n \rangle}_{=0} - k_n \underbrace{\langle x_i | x_{n-1} \rangle}_{=0} = \langle x_i | \hat{H} | x_n \rangle .$$

The hermiticity of  $\hat{H}$  yields

$$\begin{aligned}\langle x_i | \hat{H} | x_n \rangle &= \left( \langle x_n | \hat{H} | x_i \rangle \right)^* \\ &= \left( \langle x_n | (\tilde{x}_{i+1} + \varepsilon_i |x_i\rangle + k_i |x_{i-1}\rangle) \right)^* \\ &= \left( \underbrace{\langle x_n | \tilde{x}_{i+1} \rangle}_{=0} + \varepsilon_i \underbrace{\langle x_n | x_i \rangle}_{=0} + k_i \underbrace{\langle x_n | x_{i-1} \rangle}_{=0} \right)^* \\ &= 0 ,\end{aligned}$$

which shows that the constructed set of  $n+1$  vectors is indeed orthogonal.

Moreover, it shows that the Hamilton matrix is tridiagonal in the Lanczos basis:

$$H_{ij}^t = \begin{pmatrix} \varepsilon_0 & k_1 & 0 & \cdot & \cdot \\ k_1 & \varepsilon_1 & k_2 & 0 & \cdot \\ 0 & k_2 & \varepsilon_2 & k_3 & 0 \\ \cdot & 0 & k_3 & \varepsilon_3 & k_4 \\ \cdot & \cdot & 0 & k_4 & \varepsilon_4 \end{pmatrix} . \quad (15)$$

After  $L$  iterations the remaining task is the solution of the eigenvalue problem of the  $(L+1) \times (L+1)$  tridiagonal matrix  $H^t$

$$H^t \mathbf{c}^\nu = E_\nu \mathbf{c}^\nu .$$

The best approximation to the eigenvectors of the original Hamiltonian expanded in the the subspace  $\mathcal{H}_k$  spanned by the Lanczos vectors  $\{|x_0\rangle, \dots, |x_L\rangle\}$  are therefore given by

$$|\psi_\nu\rangle = \sum_{i=0}^L c_i^\nu |x_i\rangle ,$$

where the  $c'_i$  are the components of the eigenvectors of the tridiagonal matrix  $H^t$ , i. e. the expansion coefficients in the Lanczos basis.

We summarize the Lanczos algorithm

---

**Algorithm 4.1:** LANCZOS ALGORITHM(.)

---

**assign:**  $n_{\max}, N_{\text{diag}}, L, \delta$

**initialize:**

$|\tilde{x}_0\rangle$  : appropriate initial vector  
 $|x_{-1}\rangle = 0$   
 $n = 0$   
 $converged = \mathbf{false}$

**while not converged**

$k_n = \sqrt{\langle \tilde{x}_n | \tilde{x}_n \rangle}$

**if**  $k_n < \delta$  **then**  $converged = \mathbf{true}$

$|x_n\rangle = |\tilde{x}_n\rangle / k_n$

$\varepsilon_n = \langle x_n | \hat{H} | x_n \rangle$

**if**  $\text{MOD}(n, N_{\text{diag}}) = 0$  **then**

$H_t = \text{TRIDIAGONALMATRIX}(\{\varepsilon_0, \dots, \varepsilon_n\}; \{k_1 \dots k_n\})$

$\text{SOLVE EIGENVALUE-PROBLEM}(H_t; E_\nu, \mathbf{c}_\nu)$

**if**  $E_1 \dots E_L$  are converged **then**  $converged = \mathbf{true}$

**endif**

$|\tilde{x}_{n+1}\rangle = \hat{H}|x_n\rangle - \varepsilon_n|x_n\rangle - k_n|x_{n-1}\rangle$

$n = n + 1$

**if**  $n \geq n_{\max}$  **then**  $converged = \mathbf{true}$

**end while**

---

In Fig. 3 the general performance of the Lanczos method is compared with that of the Power method and that of the simple Lanczos scheme. We observe a much faster convergence of the results of the Lanczos method and, as expected, exact convergence is achieved after 10 steps.

**Remark:** it is easy to verify that a spectral shift, as in the Power method (See Sec. 4.1), has no effect on the selection of the Lanczos vectors  $|x_n\rangle$ . The spectral shift is canceled away by the Gram-Schmidt orthogonalisation. Therefore, quite generally, the lanczos method converges well towards *extremal* eigenvectors, i. e. the largest and the smallest ones.

### 4.3 Dynamical Correlations

Dynamical correlations describe how a crystal reacts to weak external perturbations denoted by  $E(t)$ . Linear response theory expresses the reaction as

$$R(t) = \int_{-\infty}^t \chi(t, t') E(t') dt' \quad (16)$$

where  $\chi$  is actually a function of the time-differences

$$\chi(t, t') = \chi(t - t') .$$

The response (16) has the form of a convolution, and Fourier transformation yields a simple product

$$R(\omega) = \chi(\omega)E(\omega) . \quad (17)$$

The dynamical correlation function  $\chi(\omega)$ , or rather *susceptibility*, for zero temperature can be computed by the Lanczos procedure with little extra effort.

#### 4.3.1 Dynamic Green's functions

To every dynamical correlation function corresponds a Green's function. For an operator  $\hat{O}$  the retarded Green's function is defined by

$$\begin{aligned} \langle\langle \hat{O}(t); \hat{O}^\dagger \rangle\rangle &\stackrel{\text{def}}{=} -i \Theta(t) \langle [\hat{O}(t), \hat{O}^\dagger]_{\varepsilon=\pm 1} \rangle \\ &= -i \Theta(t) \left( \langle \hat{O}(t) \hat{O}^\dagger \rangle - \varepsilon \langle \hat{O}^\dagger \hat{O}(t) \rangle \right) , \end{aligned} \quad (18)$$

where in the second line the symbol  $\langle \rangle$  denotes the thermodynamic average

Commutator ( $\varepsilon = +1$ ) and anticommutator ( $\varepsilon = -1$ ) Green's functions depend on the operator  $\hat{O}$ . For a detailed introduction to the theory of Green's functions see e.g. [?]. At zero temperature, the average corresponds to the expectation value of the operators in the ground state  $|\psi_0\rangle$  of the many-particle system. In this we focus on  $T = 0$ . Finite temperatures will be discussed later on. For simplicity we will just evaluate the first one of the two terms within brackets in (18). The second one (the one which multiplies  $\varepsilon$ ) can be obtained in a similar way.

We proceed by inserting the Heisenberg time evolution of the operator  $\hat{O}$

$$\hat{O}(t) = e^{i\hat{H}t} \hat{O} e^{-i\hat{H}t} , \quad \hat{O} \stackrel{\text{def}}{=} \hat{O}(t=0) \quad (19)$$

into (18). Since  $|\psi_0\rangle$  is the exact ground-state with energy  $E_0$  we have

$$e^{-i\hat{H}t} |\psi_0\rangle = e^{-iE_0 t} |\psi_0\rangle \quad \text{and} \quad \langle \psi_0 | e^{i\hat{H}t} = \langle \psi_0 | e^{iE_0 t} , \quad (20)$$

we obtain

$$\begin{aligned}
\langle\langle \hat{O}; \hat{O}^\dagger \rangle\rangle_w^+ &\stackrel{\text{def}}{=} -i \int_{-\infty}^{\infty} \theta(t) e^{iw^+t} \langle \hat{O}(t) \hat{O}^\dagger \rangle dt \\
&= -i \int_0^{\infty} e^{iw^+t} \langle e^{i\hat{H}t} \hat{O} e^{-i\hat{H}t} \hat{O}^\dagger \rangle dt \\
&= -i \int_0^{\infty} e^{iw^+t} \langle \hat{O} e^{-i(\hat{H}-E_0)t} \hat{O}^\dagger \rangle dt \\
&= -i \left\langle \hat{O} \int_0^{\infty} e^{iw^+t} e^{-i(\hat{H}-E_0)t} dt \hat{O}^\dagger \right\rangle,
\end{aligned} \tag{21}$$

where  $w^+ = w + i0^+$ , with  $0^+$  an infinitesimal positive quantity necessary for the integral to converge. The integrals can be easily evaluated using

$$-i \int_0^{\infty} e^{i(w^+ - E)t} dt = \frac{1}{w^+ - E}.$$

Now, recalling that we perform the average in the ground state  $|\psi_0\rangle$ , which was obtained by a first Lanczos calculation, we obtain from (21)

$$\langle\langle \hat{O}, \hat{O}^\dagger \rangle\rangle_w^+ = \langle \psi_0 | \hat{O} \frac{1}{w^+ - (\hat{H} - E_0)} \hat{O}^\dagger | \psi_0 \rangle \tag{22}$$

### 4.3.2 Lehmann – Representation

We now insert a complete orthonormal set of eigenvectors of  $\hat{H}$  given by

$$\mathbb{I} = \sum_{\nu} |\psi_{\nu}\rangle \langle \psi_{\nu}|.$$

Then (22) can be cast into the form

$$\langle \psi_0 | \hat{O} \frac{1}{\omega^+ - (\hat{H} - E_0)} \hat{O}^\dagger | \psi_0 \rangle = \sum_{\nu} \frac{\langle \psi_0 | \hat{O} | \psi_{\nu} \rangle \langle \psi_{\nu} | \hat{O}^\dagger | \psi_0 \rangle}{\omega^+ - (E_{\nu} - E_0)}.$$

It is convenient to take as a starting Lanczos vector for a new iteration the (normalized) state obtained by applying the operator  $O^\dagger$  to the ground state:

$$|\varphi_0\rangle = \frac{\hat{O}^\dagger |\psi_0\rangle}{\sqrt{\langle \psi_0 | \hat{O} \hat{O}^\dagger | \psi_0 \rangle}} \tag{23}$$

Next we expand the eigenvectors  $|\psi_{\nu}\rangle$  in the Lanczos basis  $\{|\varphi_i\rangle\}$

$$|\psi_{\nu}\rangle = \sum_i c_i^{(\nu)} |\varphi_i\rangle, \quad \text{with } c_i^{(\nu)} = \langle \varphi_i | \psi_{\nu} \rangle$$

to obtain

$$\begin{aligned} \langle \psi_\nu | \hat{O}^\dagger | \psi_0 \rangle &= \sum_i c_i^{(\nu)*} \underbrace{\langle \varphi_i | \hat{O}^\dagger | \psi_0 \rangle}_{\sim |\varphi_0\rangle} = \sqrt{\langle \psi_0 | \hat{O} \hat{O}^\dagger | \psi_0 \rangle} \sum_i c_i^{(\nu)*} \underbrace{\langle \varphi_i | \varphi_0 \rangle}_{\delta_{i,0}} \\ &= \sqrt{\langle \psi_0 | \hat{O} \hat{O}^\dagger | \psi_0 \rangle} c_0^{(\nu)*}. \end{aligned}$$

This means that except of the first terms all summands vanish. Thus (22) can be approximated by

$$\langle \psi_0 | \hat{O} \frac{1}{\omega^+ - (\hat{H} - E_0)} \hat{O}^\dagger | \psi_0 \rangle = \langle \psi_0 | \hat{O} \hat{O}^\dagger | \psi_0 \rangle \sum_{\nu=1}^{N_L} \frac{|c_0^{(\nu)}|^2}{\omega^+ - (\tilde{E}_\nu - \tilde{E}_0)}, \quad (24)$$

where only the first components  $c_0^{(\nu)}$  of the expansion of the eigenvector  $|\psi_\nu\rangle$  in the Lanczos basis are required. The second term in (18) is obtained in a similar way by using an different Lanczos starting vector, namely the normalized  $\hat{O}|\psi_0\rangle$ .

- In general, the eigenstates  $|\psi_\nu\rangle$  ( $\nu = 1, \dots, N_L$ ), computed by the Lanczos procedure, do not form a complete set of basis vectors, nor are the respective energies  $\tilde{E}_\nu$  exact eigenvalues of  $\hat{H}$ .
- However, with increasing number of iterations, the Lanczos procedure converges towards the exact Green's function and the convergency can be monitored and stopped as soon as the desired accuracy is reached.
- The approximate Lehmann representation (24) is an explicit sum of simple poles.

## References

- [1] A. Harris and R. Lang, Phys.Rev. **157**, 295 (1967).